

Active plasma resonance spectroscopy: Eigenfunction solutions in spherical geometry

J. Oberrath and R.P. Brinkmann

*Institute for Theoretical Electrical Engineering,
Ruhr University Bochum, D-44780 Bochum, Germany*

(Dated: March 7, 2022)

Abstract

The term *Active Plasma Resonance Spectroscopy* (APRS) denotes a class of related techniques which utilize, for diagnostic purposes, the natural ability of plasmas to resonate on or near the electron plasma frequency ω_{pe} : A radio frequent signal (in the GHz range) is coupled into the plasma via an antenna or probe, the spectral response is recorded, and a mathematical model is used to determine plasma parameters like the electron density or the electron temperature. Based on the cold plasma model, this manuscript provides the general analytic expression of the electrical admittance of a spherical shaped probe immersed into a plasma. It is derived from the matrix representation of an appropriate operator, which describes the dynamical behavior of the probe-plasma system. This dynamical operator can be split into a conservative operator and a dissipative operator. It can be shown that the eigenvalues of the conservative operator represent the resonance frequencies of the probe-plasma system which are simply connected to the electron density. As an example, the result is applied to the spherical impedance probe and the multipole resonance probe.

I. INTRODUCTION

The term “active plasma resonance spectroscopy” denotes a number of similar plasma diagnostic methods, which exploit the natural ability of plasmas to resonate at or close to the plasma frequency of electrons. The principle is quite simple: An electrical signal in the GHz range is coupled to the plasma via an electrical probe. The spectrum of the response of the plasma is recorded, and then evaluated based on a specific mathematical model. From the structure of the spectrum one is able to calculate the electron density and maybe other plasma parameters. Clearly, the quality of the method strongly depends on the quality and reliability of the model in use.

One particular class of the method is that of electrostatic probes [1–8]. Within this class the coupling of a surface wave to the plasma is utilized, which excites resonance modes of frequencies below the electron plasma frequency. A number of different approaches has been reported to provide a deeper understanding of the resonance behavior of the system [9–24]. All of them are based on a fluid dynamical approach and restricted to specific probe designs.

However, a more general description has been provided by members of our own group [25]. There, the whole class of electrostatic probes is analyzed by means of functional analytic (Hilbert space) methods. These methods are particular suited because explicit informations on the probe geometry or the electrical operation do not enter in the description. The most important result is given by the interpretation of a complex term as the electrical admittance of the probe-plasma system. The complex term refers to the resolvent of the dynamical operator that describes the system. This interpretation relies on a justified comparison to the admittance of an electrical lumped element series resonator.

In this paper, the general expression of the electrical admittance of a spherical shaped probe is derived based on the matrix representation of the dynamical operator. This operator can be split into a conservative and a dissipative operator. We show that the eigenvalues of the conservative operator represent the resonance frequencies of the probe-plasma system. These resonance frequencies are simply connected to the electron plasma density. As an example, the result is applied to a) the spherical impedance probe (IP) investigated by Blackwell et al. [5] and b) the multipole resonance probe (MRP) [8].

II. MODEL OF AN ELECTROSTATIC PROBE OF ARBITRARY SHAPE

In a recent paper a general model of an electrostatic probe is derived and analyzed [25]. For details we refer this work. Here, we summarize the most important aspects and results: The plasma chamber (see figure 1) is given as a simply connected, spatially bounded domain \mathcal{V} , most of which is plasma (a simply connected subdomain \mathcal{P}). Other subdomains of \mathcal{V} are the plasma boundary sheath \mathcal{S} , which shields the plasma from all material objects, and possibly dielectric domains \mathcal{D} . The boundary $\partial\mathcal{V}$ of the domain \mathcal{V} is either grounded (\mathcal{G}) or ideally insulating (\mathcal{I}) with vanishing conductivity and permittivity.

Into this idealized plasma chamber an arbitrarily shaped probe is immersed. The probe contains a finite number of powered electrodes \mathcal{E}_n , $n = 1 \dots N$, which are insulated from each other and from ground. The electrodes are driven by rf voltages U_n . Grounded surfaces can be treated as another electrode \mathcal{E}_0 . A possible dielectric shielding of the probe is represented as a part of the subdomain \mathcal{D} within the plasma chamber \mathcal{V} .

Within the subdomain \mathcal{P} , the dynamical behavior of the plasma, given by the dynamics of the charge density ρ_e and the current density \mathbf{j}_e , is appropriately described by the cold plasma model in electrostatic approximation. Assuming a complete electron depletion within the sheath \mathcal{S} , a surface charge density σ_e at the sheath edge \mathcal{K} has to be taken into account. The corresponding equations, including the constant plasma frequency ω_{pe} and the collision frequency for electron-neutral-collisions ν is given by

$$\begin{aligned} \frac{\partial\sigma_e}{\partial t} &= -\mathbf{n} \cdot \mathbf{j}_e \Big|_{\mathbf{r} \in \mathcal{K}} , \\ \frac{\partial\rho_e}{\partial t} &= -\nabla \cdot \mathbf{j}_e , \\ \frac{\partial\mathbf{j}_e}{\partial t} &= -\varepsilon_0\omega_{pe}^2 \nabla\phi - \nu\mathbf{j}_e - \varepsilon_0\omega_{pe}^2 \sum_{n=1}^N U_n \nabla\psi_n . \end{aligned} \tag{1}$$

ϕ is the inner electrostatic potential and is governed by Poisson's equation in the domain \mathcal{V} subject to homogeneous boundary conditions

$$-\nabla \cdot (\varepsilon_0\varepsilon_r \nabla\phi) = \begin{cases} 0 & \mathbf{r} \in \mathcal{D} \cup \mathcal{S} \\ \sigma_e & \mathbf{r} \in \mathcal{K} \\ \rho_e & \mathbf{r} \in \mathcal{P} \end{cases} . \tag{2}$$

The functions ψ_n , representing the vacuum coupling between the electrodes, are solutions to the homogeneous Poisson equation,

$$-\nabla \cdot (\varepsilon_0 \varepsilon_r \nabla \psi_n) = 0 . \quad (3)$$

They contain information about the geometry and satisfy the boundary conditions $\psi_n = \delta_{nn'}$ at the electrodes \mathcal{E}_n , with $\delta_{nn'}$ being Kronecker's delta. The respective permittivity ε_r is given as 1 within the \mathcal{S} and \mathcal{P} and with $\varepsilon_D = \text{const}$ within \mathcal{D} .

The dynamical equations (1) can be written in matrix form. This allows to interpret σ_e , ρ_e , and \mathbf{j}_e as variables of the state vector $|z\rangle$, given by

$$|z\rangle = \begin{pmatrix} \sigma_e \\ \rho_e \\ \mathbf{j}_e \end{pmatrix} . \quad (4)$$

The state vector is an element of the linear vector space \mathcal{H} . For two different state vectors $|z\rangle$ and $|z'\rangle$ a scalar product, which is motivated by the inner energy, can be defined by

$$\langle z' | z \rangle = \int_{\mathcal{V}} \varepsilon \nabla \phi'^* \cdot \nabla \phi d^3r + \int_{\mathcal{P}} \frac{1}{\varepsilon_0 \omega_{pe}^2} \mathbf{j}_e'^* \cdot \mathbf{j}_e d^3r . \quad (5)$$

It is compatible with the dynamical equations and induces the corresponding norm $\|z\| = \sqrt{\langle z | z \rangle}$. By means of $\|z\|$ it is possible to show that \mathcal{H} is complete for all square integrable state vectors including singular functions like the surface charge density. Thus, \mathcal{H} is a Hilbert space.

Another important vector is the excitation vector

$$|e_n\rangle = \begin{pmatrix} 0 \\ 0 \\ -\varepsilon_0 \omega_{pe}^2 \nabla \psi_n \end{pmatrix} . \quad (6)$$

Computing the scalar product between the excitation vector and the state vector, it turns out that this scalar product is equal to the inner current i_n at the electrode \mathcal{E}_n . The inner current represents the observable response of the dynamic system and is given by

$$i_n = \langle e_n | z \rangle = - \int_{\mathcal{V}} \nabla \psi_n \cdot \mathbf{j}_e d^3r . \quad (7)$$

This result shows, that the excitation vector acts also as observation vector.

Furthermore, two operators can be identified: The conservative operator \mathbb{T}_C which is anti-hermitian and the dissipative operator \mathbb{T}_D which is hermitian and positive definite. These operators contain information about the frequency and collisional damping behavior of the system, respectively. One can find

$$\mathbb{T}_C |z\rangle = \begin{pmatrix} -\mathbf{n} \cdot \mathbf{j}_e |_{\mathbf{r} \in \mathcal{K}} \\ -\nabla \cdot \mathbf{j}_e \\ -\varepsilon_0 \omega_{pe}^2 \nabla \phi \end{pmatrix}, \quad (8)$$

$$\mathbb{T}_D |z\rangle = \begin{pmatrix} 0 \\ 0 \\ -\nu \mathbf{j}_e \end{pmatrix}. \quad (9)$$

By means of these definitions it is possible to describe the dynamical behavior of the probe-plasma system in an abstract, but very compact form

$$\frac{\partial}{\partial t} |z\rangle = \mathbb{T}_C |z\rangle + \mathbb{T}_D |z\rangle + \sum_{n=1}^N U_n |e_n\rangle. \quad (10)$$

Concerning measurements, the stationary solutions lie on the focus of interest. Therefore, a harmonic ansatz with the frequency ω_{RF} is adequate to solve the dynamic equation for the state vector,

$$|z\rangle = \sum_{n=1}^N \frac{U_n}{i\omega_{RF} - \mathbb{T}_C - \mathbb{T}_D} |e_n\rangle. \quad (11)$$

Entering the general solution of the state vector (11) into the expression (7), one finds that the current i_n is given by the resolvent of the complete dynamical operator $\mathbb{T}_C + \mathbb{T}_D$

$$i_n = \langle e_n | z \rangle = \sum_{n'=1}^N \langle e_n | \frac{1}{i\omega_{RF} - \mathbb{T}_C - \mathbb{T}_D} | e_{n'} \rangle U_{n'} = \sum_{n'=1}^N Y_{nn'} U_{n'}. \quad (12)$$

Thus, the scalar product between two excitation vectors and the resolvent can be interpreted as the admittance $Y_{nn'}$ between two electrodes,

$$Y_{nn'} = \langle e_n | \frac{1}{i\omega_{RF} - \mathbb{T}_C - \mathbb{T}_D} | e_{n'} \rangle. \quad (13)$$

The interpretation of equation (13) is the main result of the analysis of the general model in ref. [25]. Based on functional analytic methods, this result can be used to determine an approximated or analytic expression for the admittance between two arbitrary electrodes, which is not derived yet. For this purpose, a complete orthonormal basis $\{|k\rangle\}$ of the Hilbert space is needed. Two of these basis vectors are orthonormal to each other and they satisfy the completeness relation

$$\langle k' | k \rangle = \delta_{kk'} \quad , \quad \sum_k |k\rangle \langle k| = 1 . \quad (14)$$

Inserting these expressions into (13) allows to expand the admittance $Y_{nn'}$ via the orthonormal basis and yields

$$Y_{nn'} = \sum_{k'} \langle e_n | k' \rangle \sum_k \langle k' | \frac{1}{i\omega_{\text{RF}} - \mathbb{T}_C - \mathbb{T}_D} |k\rangle \langle k | e_{n'} \rangle . \quad (15)$$

One can see that the scalar product between two basis vectors and the resolvent represents the matrix elements of the resolvent's matrix representation. Based on (14) it is possible to show, that the matrix representation of the resolvent is equal to the inverse matrix representation of the operator $i\omega_{\text{RF}} - \mathbb{T}_C - \mathbb{T}_D$

$$\sum_k \langle k' | i\omega_{\text{RF}} - \mathbb{T}_C - \mathbb{T}_D |k\rangle \langle k | \frac{1}{i\omega_{\text{RF}} - \mathbb{T}_C - \mathbb{T}_D} |k'\rangle = 1 . \quad (16)$$

This result provides the opportunity to first determine the matrix representation of the operator and then to calculate its inverse to find the matrix representation of the resolvent.

Now, the solution strategy is obvious: One has to choose a set of orthonormal basis functions, after that the matrix elements of the operator $i\omega_{\text{RF}} - \mathbb{T}_C - \mathbb{T}_D$ can be determined to find the matrix of the resolvent, then the scalar products between the basis vectors and the excitation vectors have to be computed, and finally the admittance is given by a vector-matrix-vector multiplication.

In a complex geometry an appropriate set of orthonormal basis functions has to be found to determine an approximated matrix representation of the operators. This leads to an efficient calculation of an approximated admittance instead of a simulation. It can be used to determine the spectral response, e.g., of the plasma absorption probe [6]. However, in this manuscript we focus on probes with a spherical probe tip. This allows, as we will show in the following sections, to derive an analytic solution of the admittance in a spherical probe-plasma system.

III. ORTHONORMAL BASIS IN SPHERICAL GEOMETRY

As shown in the end of the last section, an orthonormal basis is needed to calculate the matrix representation of the resolvent. The ideal basis would be the eigenfunction set of the complete dynamic operator $\mathsf{T}_C + \mathsf{T}_D$. However, it is worth noting, that T_C and T_D do not commute, which means that they do not have the same set of eigenvectors. Therefore, we follow the perturbation approach for operators since the collision frequency ν in a low pressure plasma is much smaller than the frequency range of interest.

For this purpose we have to determine the eigenvectors of the conservative operator T_C . Here, we focus on spherical geometry because the idealized spherical impedance probe and the idealized multipole resonance probe have a perfectly spherical geometry. They are depicted in figure 2 with the probe radius R , the thickness of the dielectric d , and the sheath thickness δ .

Due to the fact that T_C is anti-hermitian the eigenvalue equation can be written with a pure imaginary eigenvalue $i\omega |z\rangle = \mathsf{T}_C |z\rangle$. To solve the eigenvalue problem in spherical geometry we expand all scalar functions in spherical harmonics

$$\begin{aligned}\sigma_e(\vartheta, \varphi) &= \sum_{l=0}^{\infty} \sum_{m=-l}^l \sigma_{lm} Y_{lm}(\vartheta, \varphi) , \\ \rho_e(r, \vartheta, \varphi) &= \sum_{l=0}^{\infty} \sum_{m=-l}^l \rho_{lm}(r) Y_{lm}(\vartheta, \varphi) , \\ \phi(r, \vartheta, \varphi) &= \sum_{l=0}^{\infty} \sum_{m=-l}^l \phi_{lm}(r) Y_{lm}(\vartheta, \varphi) ,\end{aligned}\tag{17}$$

and the current density in vectorial spherical harmonics

$$\mathbf{j}_e(r, \vartheta, \varphi) = \sum_{l=0}^{\infty} \sum_{m=-l}^l j_{lm}^{(X)}(r) \mathbf{X}_{lm}(\vartheta, \varphi) + j_{lm}^{(Y)}(r) \mathbf{Y}_{lm}(\vartheta, \varphi) + j_{lm}^{(Z)}(r) \mathbf{Z}_{lm}(\vartheta, \varphi) .\tag{18}$$

This expansion leads to the following set of equations:

$$i\omega\sigma_{lm} = -j_{lm}^{(Y)} \Big|_{r=R+\delta} ,\tag{19}$$

$$i\omega\rho_{lm} = - \left[\frac{1}{r^2} \frac{\partial}{\partial r} \left(r^2 j_{lm}^{(Y)} \right) - \frac{i}{r} \sqrt{l(l+1)} j_{lm}^{(Z)} \right] ,\tag{20}$$

$$i\omega j_{lm}^{(X)} = 0 ,\tag{21}$$

$$i\omega j_{lm}^{(Y)} = -\varepsilon_0 \omega_{pe}^2 \frac{\partial}{\partial r} \phi_{lm} ,\tag{22}$$

$$i\omega j_{lm}^{(Z)} = \varepsilon_0 \omega_{pe}^2 \frac{i}{r} \sqrt{l(l+1)} \phi_{lm} .\tag{23}$$

Consequently, Poisson's equation reads

$$-\varepsilon_0 \left[\frac{1}{r^2} \frac{\partial}{\partial r} \left(r^2 \frac{\partial}{\partial r} \phi_{lm} \right) - \frac{l(l+1)}{r^2} \phi_{lm} \right] = \begin{cases} 0 & r \in [R-d, R+\delta) \\ \sigma_{lm} & r = R+\delta \\ \rho_{lm} & r \in [R+\delta, \infty) \end{cases} \quad (24)$$

with the corresponding boundary conditions

$$\phi_{lm}^{(\mathcal{D})}(R-d) = 0 \quad \text{and} \quad \lim_{r \rightarrow \infty} \phi_{lm}^{(\mathcal{P})}(r) = 0, \quad (25)$$

and transition conditions

$$\begin{aligned} \phi_{lm}^{(\mathcal{D})}(R) - \phi_{lm}^{(\mathcal{S})}(R) &= 0, & \phi_{lm}^{(\mathcal{P})}(R+\delta) - \phi_{lm}^{(\mathcal{S})}(R+\delta) &= 0, \\ \left(\varepsilon_D \frac{\partial \phi_{lm}^{(\mathcal{D})}}{\partial r} - \frac{\partial \phi_{lm}^{(\mathcal{S})}}{\partial r} \right) \Big|_{r=R} &= 0, & -\varepsilon_0 \left(\frac{\partial \phi_{lm}^{(\mathcal{P})}}{\partial r} - \frac{\partial \phi_{lm}^{(\mathcal{S})}}{\partial r} \right) \Big|_{r=R+\delta} &= \sigma_{lm}. \end{aligned} \quad (26)$$

From (19) to (23) it is obvious that two cases have to be distinguished: $\omega = 0$ and $\omega \neq 0$. Indeed $\omega = 0$ is an eigenvalue of the operator \mathbb{T}_C , but it is not excited by the harmonic RF voltages applied to the electrodes of the probe. Due to that it has no contribution to the response function and will not be considered in the rest of the manuscript. The case $\omega \neq 0$ is more important. Combining the dynamical equations (20), (22), and (23) with Poisson's equation (24) one obtains

$$\left(1 - \frac{\omega_{pe}^2}{\omega^2} \right) \left[\frac{1}{r^2} \frac{\partial}{\partial r} \left(r^2 \frac{\partial}{\partial r} \phi_{lm}^{(\mathcal{P})} \right) - \frac{l(l+1)}{r^2} \phi_{lm}^{(\mathcal{P})} \right] = 0. \quad (27)$$

And again, two cases can be distinguished: $\omega = \pm\omega_{pe}$ and $\omega \neq \pm\omega_{pe}$.

Since for $\omega \neq \pm\omega_{pe}$, the potential in the plasma has to satisfy Laplace's equation. The same holds of course for the potential in \mathcal{D} and \mathcal{S} . Thus, all potentials are governed by the same equation because the permittivity is constant in the different regions

$$\frac{1}{r^2} \frac{\partial}{\partial r} \left(r^2 \frac{\partial}{\partial r} \phi_{lm}^{(\mathcal{D},\mathcal{S},\mathcal{P})} \right) - \frac{l(l+1)}{r^2} \phi_{lm}^{(\mathcal{D},\mathcal{S},\mathcal{P})} = 0. \quad (28)$$

Its general solution is given by

$$\phi_{lm}^{(\mathcal{D},\mathcal{S},\mathcal{P})}(r) = A^{(\mathcal{D},\mathcal{S},\mathcal{P})} r^l + B^{(\mathcal{D},\mathcal{S},\mathcal{P})} r^{-(l+1)}. \quad (29)$$

The coefficients $A^{(\mathcal{S},\mathcal{P})}$ and $B^{(\mathcal{D},\mathcal{S},\mathcal{P})}$ are determined by five of the boundary and transition conditions given in (25) and (26)

$$\begin{aligned}
B^{(\mathcal{D})} &= -\frac{A^{(\mathcal{D})}}{(R-d)^{2l+1}} =: -\frac{A_{lm}}{(R-d)^{2l+1}} \\
A^{(\mathcal{S})} &= \frac{A^{(\mathcal{D})}}{2l+1} \left[1 + l(\varepsilon_D + 1) + (l+1)(\varepsilon_D - 1) \left(1 - \frac{d}{R}\right)^{2l+1} \right] =: A_{lm}A_l^{(\mathcal{S})} \\
B^{(\mathcal{S})} &= \frac{A^{(\mathcal{D})}}{2l+1} \left[l(1 - \varepsilon_D)R^{2l+1} - (l + \varepsilon_D(l+1))(R-d)^{2l+1} \right] =: A_{lm}B_l^{(\mathcal{S})} \\
A^{(\mathcal{P})} &= 0 \\
B^{(\mathcal{P})} &= \frac{A^{(\mathcal{D})}}{2l+1} \left\{ l(1 - \varepsilon_D)R^{2l+1} - (l + (l+1)\varepsilon_D)(R-d)^{2l+1} \right. \\
&\quad \left. + (R+\delta)^{2l+1} \left[(l+1)(\varepsilon_D - 1) \left(1 - \frac{d}{R}\right)^{2l+1} + 1 + l(1 + \varepsilon_D) \right] \right\} =: A_{lm}B_l^{(\mathcal{P})}
\end{aligned} \tag{30}$$

Each of these coefficients depends on $A^{(\mathcal{D})} = A_{lm}$ and they allow for the complete inner potential to be written as

$$\phi(\mathbf{r}) = \sum_{l,m} A_{lm} Y_{lm} \begin{cases} r^l - (R-d)^{2l+1} r^{-(l+1)} & , \mathbf{r} \in \mathcal{D} \\ A_l^{(\mathcal{S})} r^l + B_l^{(\mathcal{S})} r^{-(l+1)} & , \mathbf{r} \in \mathcal{S} \\ B_l^{(\mathcal{P})} r^{-(l+1)} & , \mathbf{r} \in \mathcal{P} \end{cases} . \tag{31}$$

The sixth condition given in (25) and (26) determines the eigenvalues of \mathbb{T}_C in spherical coordinates

$$\begin{aligned}
\omega_{lm} &= \pm \omega_{pe} \sqrt{\frac{l+1}{2l+1} \left[1 - \frac{l(\varepsilon_D - 1) + (\varepsilon_D(l+1) + l) \left(1 - \frac{d}{R}\right)^{2l+1}}{1 + l(1 + \varepsilon_D) + (l+1)(\varepsilon_D - 1) \left(1 - \frac{d}{R}\right)^{2l+1}} \left(1 + \frac{\delta}{R}\right)^{-(2l+1)} \right]} \\
&=: \pm \omega_{pe} \eta_l .
\end{aligned} \tag{32}$$

They are proportional to the electron plasma frequency and thus, simply connected to the electron density. It is important to note that the eigenvalues are independent of the index m . This shows that the resonance modes of a spherical probe-plasma system described by the cold plasma model are always symmetric referred to a rotation around an arbitrary rotation axis. The corresponding charge, surface charge, and current density depend on the inner potential defined by the equations (19) to (23).

In the case $\omega = \pm\omega_{\text{pe}}$ an arbitrary potential fulfills equation (27) in the plasma region

$$\phi_{lm}^{(\mathcal{P})}(r) = \text{arbitrary} , \forall \mathbf{r} \in \mathcal{P} \quad \text{with} \quad \lim_{r \rightarrow \infty} \phi_{lm}^{(\mathcal{P})}(r) = 0 . \quad (33)$$

The potential in \mathcal{S} and \mathcal{D} vanishes due to the rewritten boundary and transition conditions in this case and the complete inner potential is given by

$$\phi(\mathbf{r}) = \sum_{l,m} Y_{lm} \begin{cases} 0 & , \mathbf{r} \in \mathcal{S} \cup \mathcal{D} \\ \phi_{lm}^{(\mathcal{P})}(r) & , r \in \mathcal{P} \end{cases} . \quad (34)$$

Again, the corresponding charge, surface charge, and current density depend on the inner potential.

In summary, we find the following two different eigenvectors of the conservative operator \mathbb{T}_C , which build a complete orthogonal set in the Hilbert space

$\omega = \pm\omega_{lm}$:

$$\left| z_{lm}^{(1\pm)} \right\rangle = \begin{pmatrix} \varepsilon_0 \frac{\omega_{\text{pe}}^2}{\omega_{lm}^2} \frac{l+1}{(R+\delta)^{l+2}} Y_{lm} \\ 0 \\ \pm \varepsilon_0 \frac{\omega_{\text{pe}}^2}{\omega_{lm}} \left[-i(l+1) \mathbf{Y}_{lm} + \sqrt{l(l+1)} \mathbf{Z}_{lm} \right] \frac{B_l^{(\mathcal{P})}}{r^{l+2}} \end{pmatrix} \quad (35)$$

$\omega = \pm\omega_{\text{pe}}$:

$$\left| z_{lm}^{(2\pm)} \right\rangle = \begin{pmatrix} -\varepsilon_0 \frac{\partial}{\partial r} \phi_{lm}^{(\mathcal{P})} \Big|_{r=R+\delta} Y_{lm} \\ -\frac{\varepsilon_0}{r^2} \left[\frac{\partial}{\partial r} \left(\frac{\partial}{\partial r} \phi_{lm}^{(\mathcal{P})} \right) - l(l+1) \phi_{lm}^{(\mathcal{P})} \right] Y_{lm} \\ \pm \varepsilon_0 \omega_{\text{pe}} \left[i \frac{\partial}{\partial r} \phi_{lm}^{(\mathcal{P})}(r) \mathbf{Y}_{lm} + \frac{\sqrt{l(l+1)}}{r} \phi_{lm}^{(\mathcal{P})}(r) \mathbf{Z}_{lm} \right] \end{pmatrix} \quad (36)$$

A scalar product naturally induces a norm, whereby the eigenvectors can be normalized. In spherical geometry it is possible to simplify the scalar product (5) via the expansion in the orthogonal spherical harmonics

$$\begin{aligned} \langle z' | z \rangle &= \sum_{l,m} \int_{R-d}^{\infty} \varepsilon \left(\left| \frac{\partial \phi_{lm}}{\partial r} \right|^2 + \frac{l(l+1)}{r^2} |\phi_{lm}|^2 \right) r^2 dr \\ &+ \frac{1}{\varepsilon_0 \omega_{pe}^2} \sum_{l,m} \int_{R+\delta}^{\infty} \left(|j_{lm}^{(X)}|^2 + |j_{lm}^{(Y)}|^2 + |j_{lm}^{(Z)}|^2 \right) r^2 dr . \end{aligned} \quad (37)$$

By means of the simplified scalar product (37) each norm of the different eigenvectors can be determined. Introducing the components of the inner potential and the current density into the scalar product, the squared norm of the first eigenvector can explicitly be evaluated

$$\left\| z_{lm}^{(1)} \right\|^2 = \langle z_{lm}^{(1)} | z_{lm}^{(1)} \rangle = \frac{2\varepsilon_0(l+1)B_l^{(\mathcal{P})2}}{(R+\delta)^{2l+1}\eta_l^2} . \quad (38)$$

The elements of the second eigenvector depend on the inner potential $\phi_{lm}^{(\mathcal{P})}$ in the plasma region \mathcal{P} . It turns out that the remaining integrals in the scalar product are equal and the norm results in

$$\left\| z_{lm}^{(2)} \right\|^2 = \langle z_{lm}^{(2)} | z_{lm}^{(2)} \rangle = 2\varepsilon_0 \int_{R+\delta}^{\infty} \left[\left| \frac{\partial \phi_{lm}^{(\mathcal{P})}}{\partial r} \right|^2 + \frac{l(l+1)}{r^2} |\phi_{lm}^{(\mathcal{P})}|^2 \right] r^2 dr . \quad (39)$$

The integral remains undetermined due to the arbitrary inner potential in \mathcal{P} .

Once the norms are determined, we are able to define the following completeness relation because the normalized eigenvectors build a complete orthonormal set in the Hilbert space

$$\sum_{lm} \left(\left| \hat{z}_{lm}^{(1+)} \right\rangle \left\langle \hat{z}_{lm}^{(1+)} \right| + \left| \hat{z}_{lm}^{(1-)} \right\rangle \left\langle \hat{z}_{lm}^{(1-)} \right| + \left| \hat{z}_{lm}^{(2+)} \right\rangle \left\langle \hat{z}_{lm}^{(2+)} \right| + \left| \hat{z}_{lm}^{(2-)} \right\rangle \left\langle \hat{z}_{lm}^{(2-)} \right| \right) = 1 . \quad (40)$$

As seen in equation (15) the completeness relation is needed for the expansion and simplification of the admittance given in equation (13). Additionally, it allows the expansion of an arbitrary state vector in the eigenvectors of the conservative operator

$$|z\rangle = \sum_{l,m} A_{lm}^{(1+)} \left| \hat{z}_{lm}^{(1+)} \right\rangle + A_{lm}^{(1-)} \left| \hat{z}_{lm}^{(1-)} \right\rangle + A_{lm}^{(2+)} \left| \hat{z}_{lm}^{(2+)} \right\rangle + A_{lm}^{(2-)} \left| \hat{z}_{lm}^{(2-)} \right\rangle . \quad (41)$$

IV. GENERAL EXCITATION VECTOR

After the orthonormal basis is derived, we have to compute the excitation vector to determine the admittance (15). Based on the specified geometry we are able to calculate the general excitation vector $|e_n\rangle$. It contains the characteristic functions ψ_n , which follow Laplace's equation

$$\nabla \cdot (\varepsilon_0 \varepsilon_r \nabla \psi_n) = 0 \quad \text{with} \quad \lim_{r \rightarrow \infty} \psi_n = 0 \quad \text{and} \quad \psi_n \Big|_{\mathcal{E}_{n'}} = \delta_{nn'} . \quad (42)$$

Similar to the eigenvector calculation we expand the characteristic functions in spherical harmonics and determine the solution in r -direction

$$\psi_{lm}(r) = \begin{cases} \alpha^{(\mathcal{D})} r^l + \beta^{(\mathcal{D})} r^{-(l+1)} & , r \in [R-d, R] \\ \beta^{(\text{vac})} r^{-(l+1)} & , r \in [R, \infty) \end{cases} . \quad (43)$$

Due to the continuity of the vacuum potential and the electric flux density at the surface of the dielectric we find the following transition conditions

$$\psi_{lm}^{(\mathcal{D})}(R) = \psi_{lm}^{(\text{vac})}(R) \quad , \quad \varepsilon_D \frac{\partial}{\partial r} \psi_{lm}^{(\mathcal{D})} \Big|_R = \frac{\partial}{\partial r} \psi_{lm}^{(\text{vac})} \Big|_R . \quad (44)$$

They allow for $\alpha^{(\mathcal{D})}$ and $\beta^{(\mathcal{D})}$ to be determined dependent on $\beta^{(\text{vac})} = \beta_{lm}^{(n)}$

$$\alpha^{(\mathcal{D})} = \frac{(l+1)(\varepsilon_D - 1)}{(2l+1)\varepsilon_D R^{2l+1}} \beta^{(\text{vac})} \quad , \quad \beta^{(\mathcal{D})} = \frac{1 + l(1 + \varepsilon_D)}{(2l+1)\varepsilon_D} \beta^{(\text{vac})} . \quad (45)$$

By means of these coefficients the general characteristic functions are defined as

$$\psi_n(\mathbf{r}) = \sum_{l,m} \beta_{lm}^{(n)} \psi_{lm}^{(n)}(r) Y_{lm}(\vartheta, \varphi) \quad (46)$$

and determine the general excitation vector to

$$|e_n\rangle = \sum_{l,m} \left| 0, 0, -\varepsilon_0 \omega_{\text{pe}}^2 \beta_{lm}^{(n)} \left(\frac{\partial \psi_{lm}^{(n)}}{\partial r} \mathbf{Y}_{lm} - \frac{i}{r} \sqrt{l(l+1)} \psi_{lm}^{(n)} \mathbf{Z}_{lm} \right) \right\rangle . \quad (47)$$

The remaining coefficient $\beta_{lm}^{(n)}$ can be evaluated by the boundary condition $\psi_{lm}^{(n)}(R-d) = \delta_{nn'}$ at the electrodes \mathcal{E}_n . Utilizing the orthogonality of the spherical harmonics we find

$$\beta_{lm}^{(n)} = \frac{1}{\gamma_l} \int_{\mathcal{E}_n} Y_{lm}^*(\vartheta, \varphi) d\Omega \quad \text{with} \quad \gamma_l := \frac{(l+1)(\varepsilon_D - 1) \left(1 - \frac{d}{R}\right)^{2l+1} + 1 + l(1 + \varepsilon_D)}{(2l+1)\varepsilon_D R^{l+1} \left(1 - \frac{d}{R}\right)^{l+1}} . \quad (48)$$

The integral in $\beta_{lm}^{(n)}$ contains the information about the electrode configuration within the probe tip and has to remain undetermined until the configuration is defined.

V. GENERAL ADMITTANCE IN SPHERICAL GEOMETRY

Now, we are equipped with all the necessary elements to expand the admittance in equation (13) via the completeness relation (40) and determine the general admittance in a spherical geometry. Introducing the completeness relation (40) twice into (13) between the excitation vectors and the resolvent yields a long expression, in which scalar products between the eigenvectors and the excitation vectors appear. The scalar products between the excitation state vector and second eigenvector becomes zero and simplifies the admittance

$$\begin{aligned}
Y_{nm'} &= \sum_{lm} \sum_{l'm'} \langle e_n | \hat{z}_{lm}^{(1+)} \rangle \langle \hat{z}_{lm}^{(1+)} | (i\omega_{\text{RF}} - \mathsf{T}_C - \mathsf{T}_D)^{-1} | \hat{z}_{l'm'}^{(+)} \rangle \langle \hat{z}_{l'm'}^{(1+)} | e_{n'} \rangle \\
&+ \langle e_n | \hat{z}_{lm}^{(1+)} \rangle \langle \hat{z}_{lm}^{(1+)} | (i\omega_{\text{RF}} - \mathsf{T}_C - \mathsf{T}_D)^{-1} | \hat{z}_{l'm'}^{(1-)} \rangle \langle \hat{z}_{l'm'}^{(1-)} | e_{n'} \rangle \quad (49) \\
&+ \langle e_n | \hat{z}_{lm}^{(1-)} \rangle \langle \hat{z}_{lm}^{(1-)} | (i\omega_{\text{RF}} - \mathsf{T}_C - \mathsf{T}_D)^{-1} | \hat{z}_{l'm'}^{(1+)} \rangle \langle \hat{z}_{l'm'}^{(1+)} | e_{n'} \rangle \\
&+ \langle e_n | \hat{z}_{lm}^{(1-)} \rangle \langle \hat{z}_{lm}^{(1-)} | (i\omega_{\text{RF}} - \mathsf{T}_C - \mathsf{T}_D)^{-1} | \hat{z}_{l'm'}^{(1-)} \rangle \langle \hat{z}_{l'm'}^{(1-)} | e_{n'} \rangle .
\end{aligned}$$

The remaining scalar products between $|e_n\rangle$ and $|\hat{z}_{lm}^{(1\pm)}\rangle$ can explicitly be evaluated. They differ only in their sign and the expansion index. Thus they are given by

$$\langle e_n | \hat{z}_{lm}^{(+)} \rangle = -\frac{i\varepsilon_0\omega_{\text{pe}}(l+1)\beta_{lm}^{(n)}B_l^{(\mathcal{P})}}{\eta_l(R+\delta)^{2l+1}\|z_{lm}^{(1)}\|} = -\langle e_n | \hat{z}_{lm}^{(-)} \rangle , \quad (50)$$

$$\langle \hat{z}_{l'm'}^{(+)} | e_{n'} \rangle = \frac{i\varepsilon_0\omega_{\text{pe}}(l'+1)\beta_{l'm'}^{(n')}B_{l'}^{(\mathcal{P})}}{\eta_{l'}(R+\delta)^{2l'+1}\|z_{l'm'}^{(1)}\|} = -\langle \hat{z}_{l'm'}^{(-)} | e_{n'} \rangle . \quad (51)$$

Finally, we have to evaluate the matrix elements of the resolvent. Equation (16) shows that the matrix of the resolvent can be calculated by the inverse of the matrix of the operator $i\omega_{\text{RF}} - \mathsf{T}_C - \mathsf{T}_D$. As an example, we compute the matrix element concerning to the first term in equation (49), whereas the eigenvalue representation of the conservative operator T_C is used

$$\langle \hat{z}_{l'm'}^{(1+)} | i\omega_{\text{RF}} - \mathsf{T}_C - \mathsf{T}_D | \hat{z}_{lm}^{(1+)} \rangle = i(\omega_{\text{RF}} - \omega_{\text{pe}}\eta_l)\delta_{ll'}\delta_{mm'} - \langle \hat{z}_{l'm'}^{(1+)} | \mathsf{T}_D | \hat{z}_{lm}^{(1+)} \rangle . \quad (52)$$

The matrix elements of T_D have to be evaluated explicitly. Applying the operator T_D to $|\hat{z}_{lm}^{(1+)}\rangle$ yields a state vector with a vanishing charge contribution. Thus, the scalar product with $\langle\hat{z}_{l'm'}^{(1+)}|$ is reduced to the integral over the current components and is determined by

$$\begin{aligned} \langle\hat{z}_{l'm'}^{(1+)}|\mathsf{T}_D|\hat{z}_{lm}^{(1+)}\rangle &= -\frac{\nu\varepsilon_0\left[(l+1)(l'+1)+\sqrt{l(l+1)l'(l'+1)}\right]}{(l+l'+1)\eta_l\eta_{l'}\|z_{lm}^{(1)}\|\|z_{l'm'}^{(1)}\|(R+\delta)^{l+l'+1}}B_l^{(\mathcal{P})}B_{l'}^{(\mathcal{P})}\delta_{ll'}\delta_{mm'} \\ &=: -\nu_{ll'}\delta_{ll'}\delta_{mm'} . \end{aligned} \quad (53)$$

Entering (53) in (52) yields the complete first matrix element

$$\langle\hat{z}_{l'm'}^{(+)}|i\omega_{\text{RF}}-\mathsf{T}_C-\mathsf{T}_D|\hat{z}_{lm}^{(+)}\rangle = [i(\omega_{\text{RF}}-\omega_{\text{pe}}\eta_l)+\nu_{ll'}]\delta_{ll'}\delta_{mm'} . \quad (54)$$

The fact that T_D is represented by pure diagonal elements shows that T_C and T_D can be projected on the same subdomain with spherical harmonics as basisfunctions. Therefore, the perturbation approach becomes dispensable. Following the same calculation, we find the other matrix elements of the dynamical operator

$$\langle\hat{z}_{l'm'}^{(1-)}|\mathsf{T}_D|\hat{z}_{lm}^{(1-)}\rangle = [i(\omega_{\text{RF}}+\omega_{\text{pe}}\eta_l)+\nu_{ll'}]\delta_{ll'}\delta_{mm'} \quad (55)$$

$$\langle\hat{z}_{l'm'}^{(1+)}|\mathsf{T}_D|\hat{z}_{lm}^{(1-)}\rangle = \langle\hat{z}_{l'm'}^{(1-)}|\mathsf{T}_D|\hat{z}_{lm}^{(1+)}\rangle = -\nu_{ll'}\delta_{ll'}\delta_{mm'} . \quad (56)$$

This result shows that the operator $i\omega_{\text{RF}}-\mathsf{T}_C-\mathsf{T}_D$ is represented by a diagonal block matrix, where the block elements on the main diagonal are given by (2×2) -matrices. The inverse of such a matrix is also a diagonal block matrix with (2×2) -matrices on the main diagonal. Each block element on the diagonal is determined by the inverse of the (2×2) -matrix of the original block element.

Now, all terms in the admittance (49) are evaluated and can be introduced. Finally, we exploit the Kronecker deltas to determine the general admittance in a spherical geometry

$$Y_{nn'} = i\omega\varepsilon_0\omega_{\text{pe}}^2 \sum_{l=0}^{\infty} \sum_{m=-l}^l \frac{l+1}{(R+\delta)^{2l+1}} \frac{\beta_{lm}^{(n)}\beta_{lm}^{(n')}}{\omega_{\text{pe}}^2\eta_l^2 + i\omega_{\text{RF}}\nu - \omega_{\text{RF}}^2} . \quad (57)$$

The coefficients $\beta_{lm}^{(n)}$ and $\beta_{lm}^{(n')}$ are still not determined. They contain the information about the electrode configuration. Therefore, we have to distinguish between different probe designs and focus on the IP and the MRP in the next two sections.

VI. ADMITTANCE OF THE IMPEDANCE PROBE

In figure 2 (left) the idealized impedance probe is depicted. It contains one spherical powered electrode \mathcal{E}_1 and is, in our case, surrounded by a dielectric. The general current (12) is reduced to the current flowing to \mathcal{E}_1 , where the voltage U_1 is applied (For a shorter notation we substitute $\omega_{\text{RF}} = \omega$ in the rest of the manuscript.)

$$i_1 = Y_{11}U_1 = i\omega\varepsilon_0\omega_{\text{pe}}^2 \sum_{l=0}^{\infty} \sum_{m=-l}^l \frac{l+1}{(R+\delta)^{2l+1}} \frac{(\beta_{lm}^{(1)})^2 U_1}{\omega_{\text{pe}}^2 \eta_l^2 + i\omega\nu - \omega^2} \quad (58)$$

The specified electrode configuration allows for $\beta_{lm}^{(1)}$ to be evaluated explicitly by its definition given in (48)

$$\beta_{lm}^{(1)} = \frac{\sqrt{4\pi}}{\gamma_l} \delta_{l0} \delta_{m0} . \quad (59)$$

Entering (59) into the current (58) and exploiting the Kronecker deltas yields the admittance of the spherical impedance probe

$$Y_{\text{IP}} = \frac{4\pi\varepsilon_0\omega_{\text{pe}}^2}{(R+\delta)\gamma_0^2} \frac{i\omega}{\omega_{\text{pe}}^2 \eta_0^2 + i\omega\nu - \omega^2} = \left(\frac{1}{i\omega C_0} + \frac{i\omega + \nu}{\eta_0^2 \omega_{\text{pe}}^2 C_0} \right)^{-1} . \quad (60)$$

It describes the coupling between the electrode and ground, which is in infinite distance to the probe. Equation (60) shows that the impedance probe provides just one resonance mode with the resonance frequency ω_{00} , which is given by the eigenvalue of the conservative operator \mathbb{T}_C

$$\omega_{00} = \pm \omega_{\text{pe}} \sqrt{1 - \frac{\varepsilon_D (1 - \frac{d}{R})}{1 + (\varepsilon_D - 1) (1 - \frac{d}{R})} \left(1 + \frac{\delta}{R}\right)^{-1}} . \quad (61)$$

Neglecting the dielectric ($d = 0$ and $\varepsilon_D = 1$), the resonance frequency (61) reduces to the well known sheath resonance in spherical geometry [26]. It can also be called ‘‘monopole resonance’’ referring to the one electrode system.

Different spectra of the impedance probe will be depicted and discussed within section VIII. We will compare them to the spectra of the multipole resonance probe and discuss advantages and disadvantages. The admittance of the MRP is determined in the next section.

VII. ADMITTANCE OF THE MULTIPOLE RESONANCE PROBE

The idealized multipole resonance probe is shown in figure 2 (right). The probe consists of an upper electrode \mathcal{E}_1 and a lower electrode \mathcal{E}_2 , where the voltages U_1 and U_2 are applied, respectively. We calculate the current flowing to the electrode \mathcal{E}_1

$$i_1 = \sum_{n'=1}^2 Y_{1n'} U_{n'} = \sum_{n'=1}^2 \sum_{l=0}^{\infty} \sum_{m=-l}^l \frac{l+1}{(R+\delta)^{2l+1}} \frac{i\omega\varepsilon_0\omega_{\text{pe}}^2\beta_{lm}^{(1)}\beta_{lm}^{(n')}U_{n'}}{\omega_{\text{pe}}^2\eta_l^2 + i\omega\nu - \omega^2}. \quad (62)$$

Owing to the two different electrodes, we have to determine two coefficients $\beta_{lm}^{(1)}$ and $\beta_{lm}^{(2)}$

$$\beta_{lm}^{(1)} = \frac{\sqrt{(2l+1)\pi}}{\gamma_l} \frac{\sqrt{\pi}}{2\Gamma(1-\frac{l}{2})\Gamma(\frac{3+l}{2})} \delta_{m0}, \quad (63)$$

$$\beta_{lm}^{(2)} = \frac{\sqrt{(2l+1)\pi}}{\gamma_l} \left(\frac{2\sin(l\pi)}{l\pi(1+l)} - \frac{\sqrt{\pi}}{2\Gamma(1-\frac{l}{2})\Gamma(\frac{3+l}{2})} \right) \delta_{m0}. \quad (64)$$

The gamma function $\Gamma(1-\frac{l}{2})$, which is present in both coefficients, becomes infinity for all even $l > 0$. Furthermore, the sine vanishes for all $l > 0$. Thus, the coefficients vanish also for all even $l > 0$ and the remaining coefficients for odd $l = 2l' - 1$ can be combined

$$\beta_{lm}^{(1/2)} = \pm \frac{\sqrt{4l'-1}}{\gamma_{2l'-1}} \frac{\pi \delta_{l'2l'-1} \delta_{m0}}{2\Gamma(\frac{3}{2}-l')\Gamma(l'+1)} = \pm \beta_{2l'-1} \delta_{l'2l'-1} \delta_{m0}, \quad l' \in \mathbb{N}. \quad (65)$$

The positive sign belongs to $\beta_{lm}^{(1)}$ and the negative to $\beta_{lm}^{(2)}$. (65) shows the influence of the symmetric geometry to the resonance modes of the probe-plasma system. The even modes, instead of $l = 0$, vanish in the calculation. In the limit $l \rightarrow 0$ the coefficients become equal

$$\beta_{00}^{(1)} = \frac{\sqrt{\pi}}{\gamma_0} = \beta_{00}^{(2)}. \quad (66)$$

Introducing (65) and (66) into the current (62), the current can be simplified

$$i_1 = \sum_{l'=1}^{\infty} \frac{2l'}{(R+\delta)^{4l'-1}} \frac{i\omega\varepsilon_0\omega_{\text{pe}}^2 (\beta_{2l'-1})^2 (U_1 - U_2)}{\omega_{\text{pe}}^2\eta_{2l'-1}^2 + i\omega\nu - \omega^2} + \frac{1}{R+\delta} \frac{i\omega\varepsilon_0\omega_{\text{pe}}^2 (\beta_{00}^{(1)})^2 (U_1 + U_2)}{\omega_{\text{pe}}^2\eta_0^2 + i\omega\nu - \omega^2}. \quad (67)$$

The MRP is operated with symmetric voltages $U = U_1 = -U_2$. Owing to the electric symmetry the contribution of the zero mode vanishes and we evaluate the admittance

$$Y_{\text{MRP}} = \sum_{l'=1}^{\infty} \frac{4l'}{(R+\delta)^{4l'-1}} \frac{i\omega\varepsilon_0\omega_{\text{pe}}^2 (\beta_{2l'-1})^2}{\omega_{\text{pe}}^2\eta_{2l'-1}^2 + i\omega\nu - \omega^2} = \sum_{l'=1}^{\infty} \left(\frac{1}{i\omega C_{l'}} + \frac{i\omega + \nu}{\omega_{\text{pe}}^2\eta_{2l'-1}^2 C_{l'}} \right)^{-1}. \quad (68)$$

The second expression is identical to the admittance directly derived for the MRP [8]. It shows that only odd modes of the probe-plasma system can be excited, where again the resonance frequencies are determined by the eigenvalues $\omega_{2l'-1} = \omega_{\text{pe}}\eta_{2l'-1}$ of \mathbb{T}_C . Due to the geometric and electric symmetry the electrodes couple to each other and not to ground.

VIII. COMPARISON BETWEEN IP AND MRP

Within the last two sections the admittances of the impedance probe and multipole resonance probe are derived. Now, we compare their spectra based on the parameters of the MRP prototype: probe tip radius $R = 4$ mm, thickness of the dielectric $d = 1$ mm, and permittivity $\varepsilon_D = 4.6$ [27]. Additionally, we assume a sheath thickness of $\delta = 0.2$ mm, a plasma frequency of $\omega_{pe} = 2\pi 10^9 \text{ s}^{-1}$, and a collision frequency of $\nu = 0.015\omega_{pe}$. Figure 3 shows the corresponding spectra of both probes (IP dashed and MRP solid). Obviously, the resonance frequency of the IP is smaller than the ones of the MRP, as expected from the derived eigenvalues. Furthermore, one can see that the mode of the IP is less damped than the ones of the MRP.

The spectra depict in figure 4 are computed with a thickness of the dielectric that is equal to the sheath thickness $d = \delta = 0.2$ mm. This leads to a shift of the resonance frequencies to smaller values and to less damping of the higher modes. Due to that, the contribution of the higher modes to the spectrum is observable. Increasing the thickness of the dielectric to $d = 2$ mm yields the spectra in figure 5, where the resonance frequencies are shifted to higher frequencies. The higher modes of the multipole resonance probe are not observable anymore.

Both probes provide spectra with a dominant resonance peak. The monopole mode of the impedance probe is unique and just slightly damped by an increasing thickness of the dielectric. This allows a measurement also in a plasma with higher collision frequencies. However, the fact that the current couples to ground at infinity means that the interpretation of a measurement based on the excitation of the resonance mode has to be understood as an average reaction of the whole plasma. Therefore, the measurement is not local, which can be seen as a disadvantage of the impedance probe. Another advantage is the simple design.

Choosing an optimized thickness of the dielectric for the multipole resonance probe, the higher modes are strongly damped. This yields an uniquely observable dipole mode, as done for the prototype. In principle the MRP acts like a dipole with a rapid decreasing electric field, which provides a local measurement but the design is more complex to ensure the geometrical and electrical symmetry.

IX. SUMMARY AND CONCLUSION

Based on the result that the admittance of an electrostatic probe in arbitrary geometry is given by the resolvent of the dynamical operator $\mathbb{T}_C + \mathbb{T}_D$, we derived the general admittance in spherical geometry. Therefore, we determined the matrix representation of the resolvent by the eigenvalues and eigenfunctions of the conservative operator \mathbb{T}_C . In general, the operators \mathbb{T}_C and \mathbb{T}_D do not commute. However, in spherical geometry they can be projected on the same subdomain with spherical harmonics as basisfunctions. This allows for the exact analytical representation of the general admittance in spherical geometry.

Two different probe designs were chosen to compare the general admittance with established results: The spherical impedance probe and the multipole resonance probe. In both cases we showed that the admittances are simplified expressions of the general admittance. The corresponding resonance frequencies are given by the eigenvalues of the conservative operator \mathbb{T}_C , respectively. Concerning the impedance probe, the resonance frequency is equal to the sheath resonance and might also be called monopole resonance. The admittance of the multipole resonance probe is identical to the admittance, which is derived directly for the specific design [8].

Both probe designs provide spectra with a dominant resonance peak which is clearly detectable in a measurement. The impedance probe has a simple design and due to that always a unique resonance, but the measurement is not local. The multipole resonance probe has a more complex design to ensure the geometrical and electrical symmetry. Due to that symmetry the MRP acts like a dipole with a rapidly decreasing field, that the measurement is local.

The analytic solution presented here is restricted to spherical geometry. However, the solution strategy can also be performed in an arbitrary geometry. Therefore, an appropriate set of orthonormal basis functions has to be found to determine an approximated matrix representation of the operators. This will lead to an efficient calculation of the approximated spectral response instead of a simulation. Possibly, a perturbation approach is useful to determine the admittance by the matrix representation of the resolvent.

Acknowledgments

The authors acknowledge the support by the Federal Ministry of Education and Research (BMBF) in frame of the project PluTO, and also the support by the Deutsche Forschungsgemeinschaft (DFG) via Graduiertenkolleg GK 1051, Collaborative Research Center TRR 87, and the Ruhr University Research School. Gratitude is expressed to M Lapke, C Schulz, R Storch, T Styrnoll, P Awakowicz, T Musch, and I Rolfes, who are part of the MRP-Team at the Ruhr University Bochum.

-
- [1] K. Takayama, H. Ikegami, und S. Miyazaki, *Phys. Rev. Lett.* **5**, 238 (1960).
- [2] A. M. Messiaen and P. E. Vandenplas, *J. Appl. Phys.* **37**, 1718 (1966)
- [3] J. A. Waletzko and G. Bekefi, *Radio Sci.* **2**, 489 (1967).
- [4] N. Vernet, R. Manning, and J. L. Steinberg, *Radio Sci.* **10**, 517 (1975).
- [5] D. D. Blackwell, D. N. Walker, and W. E. Amatucci, *Rev. Sci. Instrum* **76**, 023503 (2005).
- [6] H. Kokura, K. Nakamura, I.P. Ghanashev, and H. Sugai, *Japan. J. Appl. Phys* **38**, 5262 (1999).
- [7] C. Scharwitz, M. Böke, J. Winter, M. Lapke, T. Mussenbrock, and R. P. Brinkmann, *Appl. Phys. Lett.* **94**, 011502 (2009).
- [8] M. Lapke, T. Mussenbrock, and R. P. Brinkmann, *Appl. Phys. Lett.* **93**, 051502 (2008).
- [9] J. A. Fejer, *Radio Sci.* **68D**, 1171 (1964)
- [10] R. S. Harp, *Appl. Phys. Lett.* **4**, 186 (1964)
- [11] R. S. Harp and F. W. Crawford, *J. Appl. Phys.* **35**, 3436 (1964)
- [12] T. Dote and T. Ichimiya, *J. Appl. Phys.* **36**, 1866 (1965).
- [13] R. J. Kostelnicek, *Radio Sci.* **3**, 319 (1968).
- [14] A. J. Cohen and G. Bekefi, *Phys. Fluids* **14**, 1512 (1971).
- [15] J. Tarstrup and W. J. Heikkila, *Radio Sci.* **4**, 493 (1972).
- [16] T. Aso, *Radio Sci.* **8**, 139 (1973).
- [17] C. C. Bantin and K. G. Balmain, *Can. J. Phys.* **52**, 291 (1974).
- [18] S. Dine, J.P. Booth, G.A Curley, C.S. Corr, J. Jolly, and J. Guillon, *Plasma Sources Sci. Technol.* **14**, 777 (2005).
- [19] D. N. Walker, R. F. Fernsler, D. D. Blackwell, W. E. Amatucci, and S. J. Messer, *Phys. Plasmas* **13**, 032108 (2006).
- [20] M. Lapke, T. Mussenbrock, R. P. Brinkmann, C. Scharwitz, M. Böke, and J. Winter, *Appl. Phys. Lett.* **90**, 121502 (2007).
- [21] J. Xu, K. Nakamura, Q. Zhang, and H. Sugai, *Plasma Sources Sci. Technol.* **18** 045009, (2009).
- [22] J. Xu, J. Shi, J. Zhang, Q. Zhang, K. Nakamura, and H. Sugai, *Chinese Phys. B* **19** 075206, (2010).
- [23] B. Li, H. Li, Z. Chen, J. Xie G. Feng, and W. Liu, *Plasma Sci. Technol.* **12**, 513 (2010).

- [24] I. Linag, K. Nakamura, and H. Sugai, *Appl. Phys. Express* **4**, 066101 (2011)
- [25] M. Lapke, J. Oberrath, T. Mussenbrock und R. P. Brinkmann, *Plasma Sources Sci. Technol.* **22**, 025005 (2013).
- [26] R. S. Harp, *Appl. Phys. Lett.* **4**, 186 (1964).
- [27] M. Lapke et al., *Plasma Sources Sci. Technol.* **20** 042001, (2011).

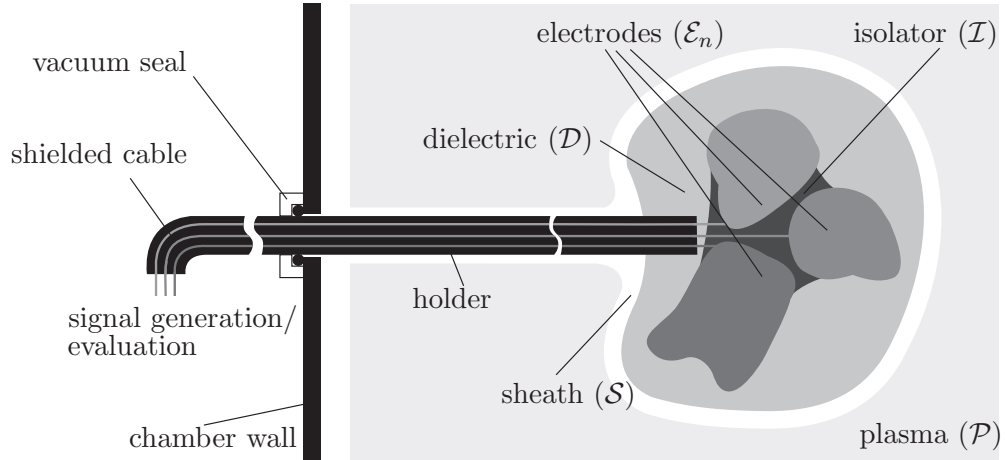


FIG. 1: Illustration of the abstract model for a N -electrode system [25] (reprint). The electrodes are shielded to each other and the plasma by some dielectric medium. The whole probe, surrounded by a plasma sheath is immersed in a plasma volume.

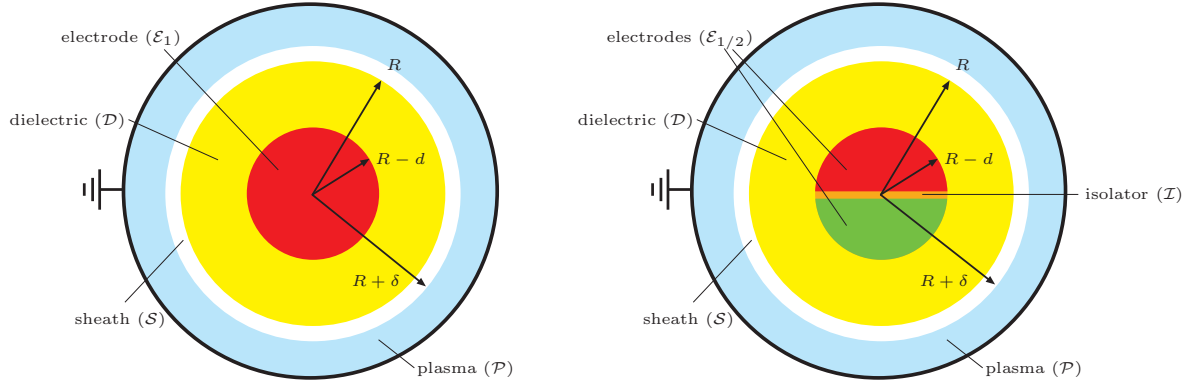


FIG. 2: Idealized impedance probe (left) and multipole resonance probe (right) with the probe radius R , thickness of the dielectric d and sheath thickness δ .

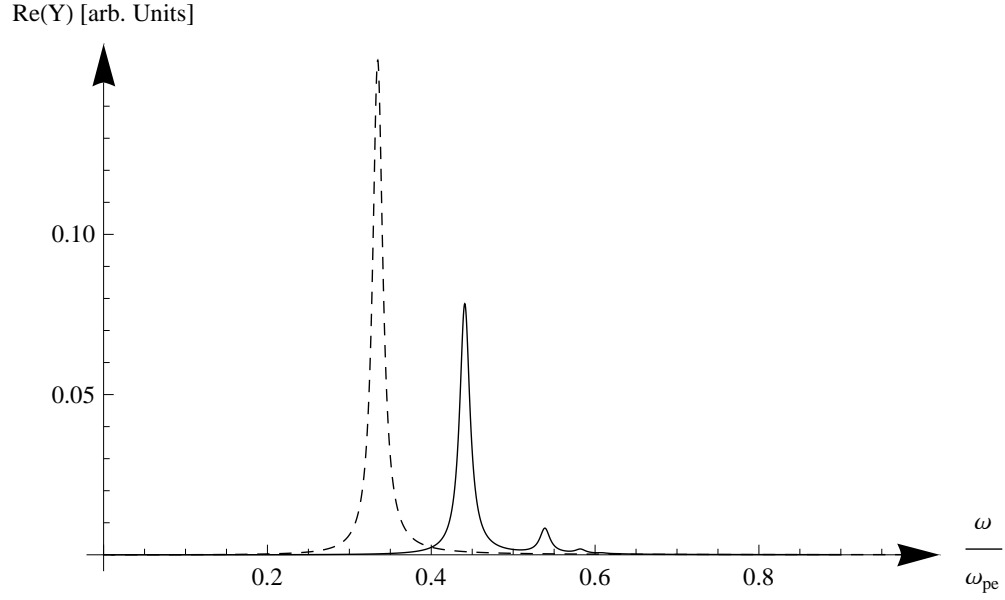


FIG. 3: Spectra of the impedance probe (dashed) and multipole resonance probe (solid) with the prototype parameter of the MRP $R = 4$ mm, $d = 1$ mm, $\varepsilon_D = 4.6$ and assumed plasma parameter $\delta = 0.2$ mm, $\omega_{pe} = 2\pi 10^9$ s $^{-1}$, $\nu = 0.015\omega_{pe}$.

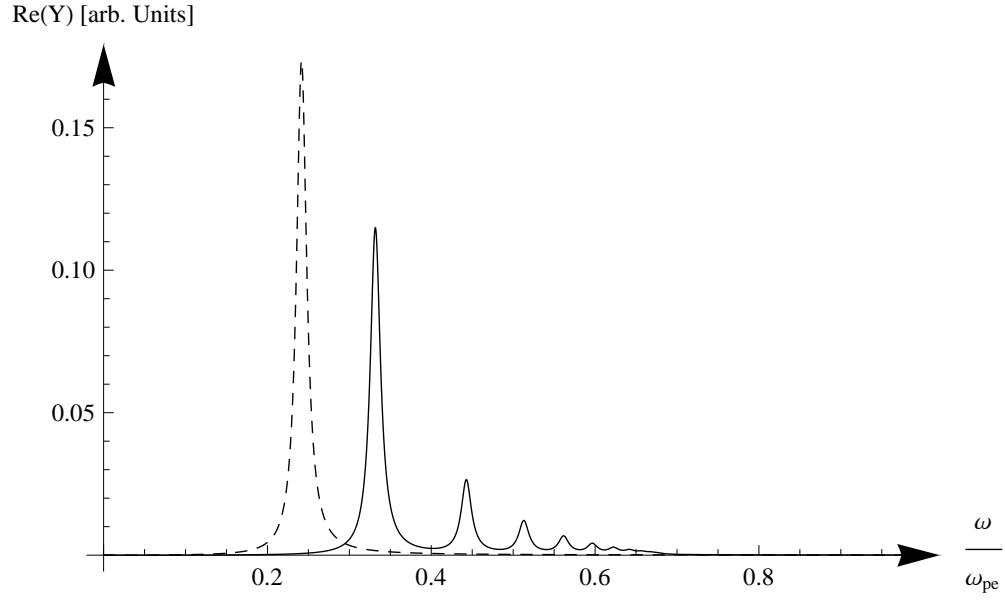


FIG. 4: Spectra of the impedance probe (dashed) and multipole resonance probe (solid) with the probe parameter $R = 4$ mm, $d = 0.2$ mm, $\varepsilon_D = 4.6$ and assumed plasma parameter $\delta = 0.2$ mm, $\omega_{pe} = 2\pi \cdot 10^9$ s $^{-1}$, $\nu = 0.015\omega_{pe}$ and .

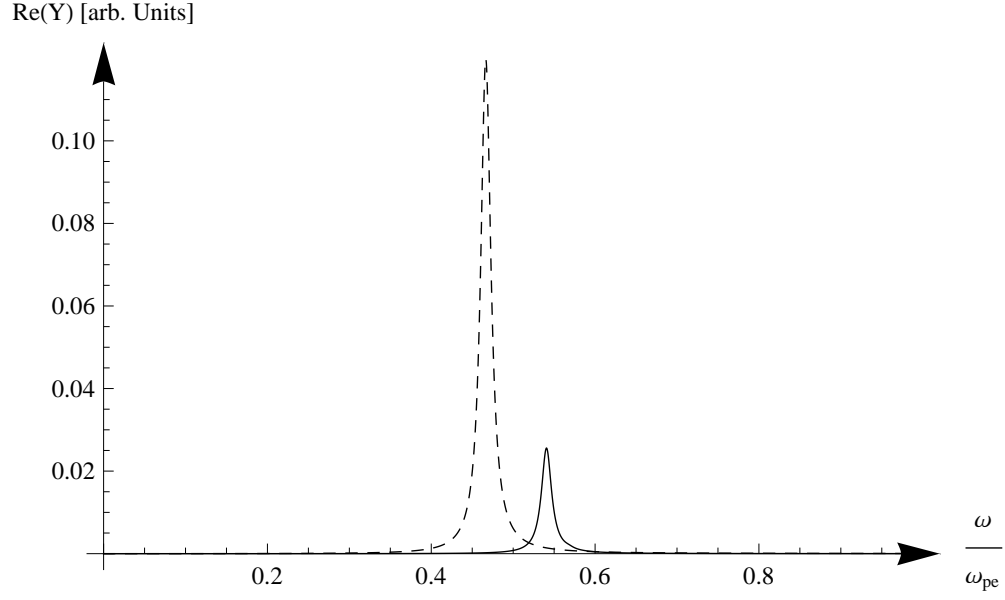


FIG. 5: Spectra of the impedance probe (dashed) and multipole resonance probe (solid) with the probe parameter $R = 4$ mm, $d = 2$ mm, $\varepsilon_D = 4.6$ and assumed plasma parameter $\delta = 0.2$ mm, $\omega_{pe} = 2\pi 10^9$ s $^{-1}$, $\nu = 0.015\omega_{pe}$.